i

INVESTIGATIONS OF ELECTRON EMISSION CHARACTERISTICS OF LOW WORK FUNCTION SURFACES

Report No. 5

by

L. W. Swanson
A. E. Bell
L. C. Crouser

Prepared for

Headquarters
National Aeronautics and Space Administration
Washington, D. C.

Quarterly Report No. 5
1 October to 31 December 1965

January 1966

CONTRACT NASw-1082

FIELD EMISSION CORPORATION
Melrose Avenue at Linke Street
McMinnville, Oregon 97128

TABLE OF CONTENTS

LIST OF ILLUSTRATIONS

PURPOSE

The primary aims of this investigation are to obtain an improved fundamental understanding of (1) the phenomena governing the production of low work function surfaces, and (2) the factors affecting the quality and stability of electron emission characteristics. It is expected that the information generated from this investigation will be relevant to various kinds of electron emission (i.e., photo, thermionic and field emission), although the primary emphasis will be placed upon field emission. Accordingly, field emission techniques will be employed, at least initially, to obtain the objectives of this work.

The formation of low work function surfaces will be accomplished by; (1) adsorption of appropriate electro-positive adsorbates, (2) co-adsorption of appropriate electro-positive and electro-negative adsorbates, and (3) fabrication of emitters of low work function surfaces from various metalloid compounds. Various properties of these surfaces to be investigated in order to obtain a more fundamental understanding of them are the temperature dependency of the emission and work function, the various types of energy exchanges accompanying emission, the energy distribution of the field emitted electron, and various aspects of the surface kinetics of adsorbed layers such as binding energy, surface mobility and effect of external fields.

ABSTRACT

A fixed orientation probe tube has been used to investigate work function change caused by localized adsorption of cesium on tungsten. Desorption in the presence of an applied electric field provided a nearly uniform coverage over the emitting area of the tip without necessitating equilibration. A new versatile probe tube has been constructed and its associated experimental program is described in this report.

More refined energy distribution and work function measurements on the (310) plane are reported. The results indicate reasonably close agreement between experiment and theory. A measurement of I-V characteristics along various (310) directions enabled us to obtain information regarding the variation of field and linear magnification with emitter apex angle.

PROGRESS TO DATE

A versatile probe tube incorporating both an oxygen and a cesium source has been designed and constructed during this quarter. The versatility of the tube arises from the fact that it is suitable both for work function and energy distribution measurements on any plane; moreover, the tube contains both a cesium and an oxygen source so that the above measurements may be carried out on single or coadsorbed layers of the above adsorbates.

In experiments performed with a fixed orientation probe tube, data has been collected which illustrates how an electric field present during cesium dosing affects the variation of work function versus dose number.

THE MAGNETIC DEFLECTION PROBE TUBE

A diagram of the tube is shown in Figure 1. The electron collector design is based on a design Dr. van Oostrom of the Phillips Laboratory, Eindhoven. It differs from earlier probe tube designs by Müller, et al in that it contains a lens electrode E. Electrons passing through the lens are focused near the center of the spherical collector F, and subsequently travel to the spherical electron collector along radius vector paths. This feature of the design enables the tube to be used successfully in total energy analyzing experiments. The envelope construction enables the main electrode assembly to be removed for inspection or alteration simply by making one crack in the aluminum-silicate glass which is conductivized on the inside only in the vicinity of the anode D. In order to minimize the electrical noise pickup by the electron collector lead as it emerges from the tube, the lead is enclosed by a molybdenum cylinder which connects directly to the shield of the co-axial cable leading to the electrometer.

The oxygen and cesium sources are arranged perpendicular to themselves and to the emitter axis and each supplies the emitter with adsorbates along a very small glass constriction which points toward the tip. Deflection
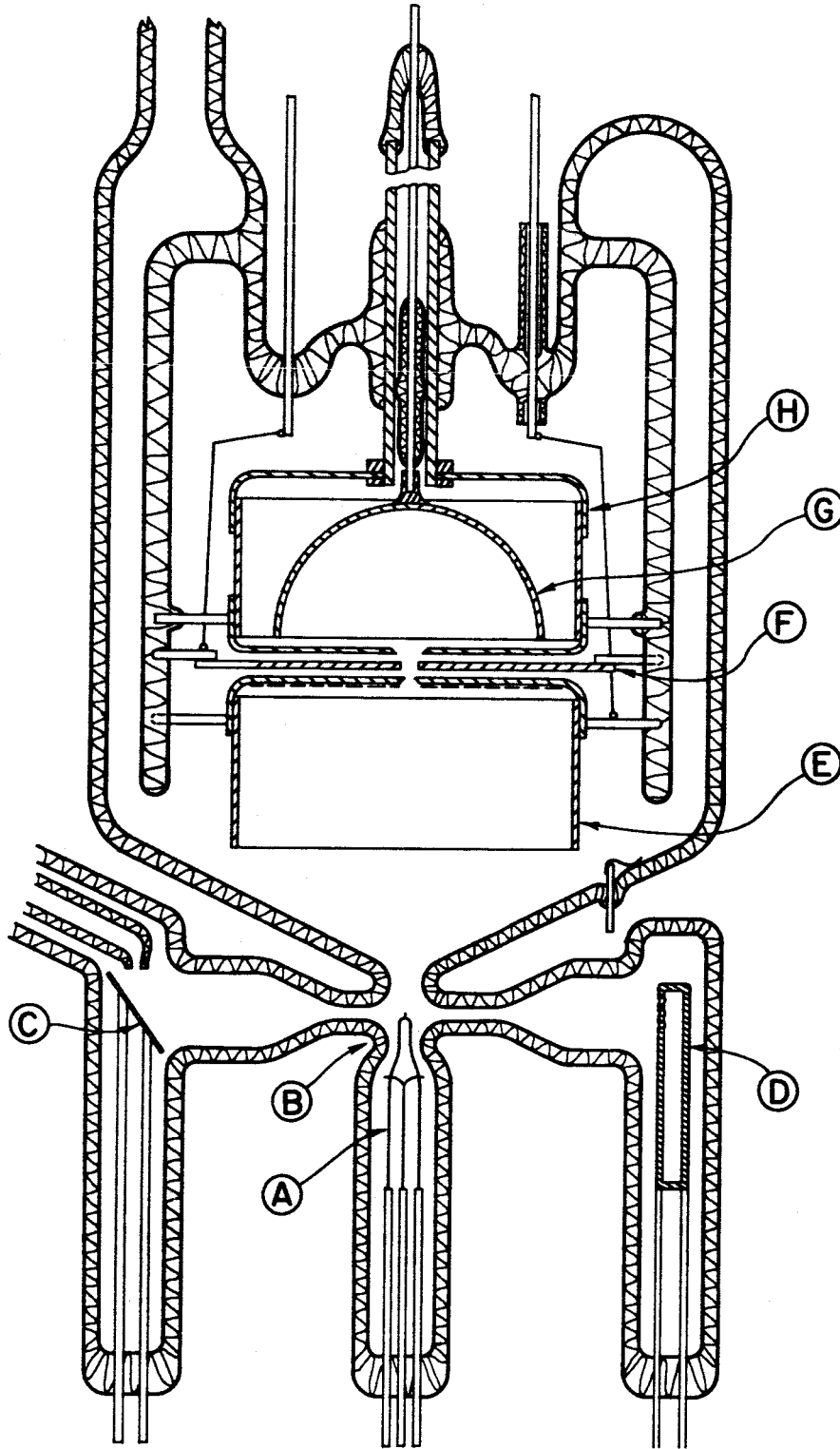
3

Figure 1.   Diagram of coadsorption magnetic deflection probe tube. Tube
contains following components:

(A) emitter assembly   (E) anode
(B) space for electromagnet (F) lens electrode
(C) cesium source platform   (G) spherical collector
(D) oxygen source   (H) Faraday cage

of the field emission electron beam is to be effected magnetically.

A mechanical method of deflecting the electron beam current was also considered; however, a simple method of deflecting the emitter is unsatisfactory because unless the emitter is swiveled about its apex, the electron beam will not enter the electrode assembly perpendicular to the anode face. Failure to do so would result in erroneous work function data. Mechanical arrangements that orient the emitter about its apex are quite complicated although such a beam deflection arrangement may be superior in energy distribution analyses since possible disturbing magnetic fields may be removed during measurements.

The deflection method employs a small quadrupole electromagnet constructed to fit snugly against the constricted part of the emitter glass envelope so that the horizontal axis through two opposite pole faces bisects that of the other pair at the emitter apex. The electromagnets have carefully annealed armco cores while all other parts of the magnet assembly are constructed of non-magnetic material. It is hoped that this will result in the absence of residual magnetic fields so that the probe beam will always be derived from the same crystallographic region of the emitter when the electromagnet current is switched off. In an earlier magnetic deflection probe tube, it was found necessary to compensate for the beam deflection resulting from alteration of the anode voltage which takes place during I, V data collection. The beam deflection under these circumstances is a consequence of the fact that electron deflection by a magnetic field is proportional to electron velocity which in the field emission tube will depend upon anode accelerating voltage.

Procedures for measuring and calculating energy distributions are described in an earlier report No. 2 of this series [1].

FUTURE EXPERIMENTAL PROGRAM

Coadsorbed layers. Composite cesium and oxygen layers are of interest in this program because of their exceptionally low work function when

5

constituted in the correct proportions. A detailed study of the average

work function and pattern changes together with the temperatures of

migration of cesium over oxygen or tungsten has been described in an

earlier report[2]. The outstanding features of this work were:

(1) the low work function (1.15 e.v.) that could be attained if the emitter

was initially heavily dosed with oxygen,

(2) the enhanced stability of the cesium layer brought about by the presence

of underlying oxygen,

(3) the sharp increase in the temperature required to spread cesium

over an oxygenated tungsten surface compared with a clean surface.

(4) although the 110 plane emits preferentially over the 100 and 211 planes

in the case of cesium on clean tungsten, the reverse is true for cesium

adsorbed on oxygenated tungsten if insufficient cesium is present to

allow attainment of the work function minimum.

The new probe tube will be utilized in making a more detailed inves-

tigation of the above features of the single and mixed adsorbate systems.

Since the average work function is heavily weighted toward that of the lowest

work function area of the emitter, information about the work functions of

the weakly emitting areas of the tip is only accessible by using probe techniques.

Energy Distribution Measurements. It is of interest to investigate the effect

of increasing amounts of adsorbed cesium on the half width $d_{1/2}$ of the electron

energy distribution. At $T = 0$, a closed expression can be obtained which maps

out the dependence of $d_{1/2}$ on work function $\emptyset$ through the parameter d:

$$d_{1/2} = 2 \times 3 \ d \log \ 2/(1 + e^{-\frac{E_f}{d}})$$

where $d = \dfrac{\hbar e F}{2 (2m \ \emptyset)^{1/2} t(y)}$, the other terms have been defined in an

earlier report of this series[3]. No such closed expression is obtained for $T \neq 0$.

Hence variation of $d_{1/2}$ at low temperatures through addition of cesium should be

determined by the effect of the cesium on work function alone. Whether or not

such a relationship holds especially at $\emptyset_{min}$ for the Cs/W system and for the

mixed adsorbate system Cs-O-W will be interesting to ascertain. Other interesting questions arise from the results obtained from the 100 direction of clean tungsten. In this case an anomalous hump was found in the energy distribution curve which has been attributed to the details of the tungsten energy band structure in the 100 direction. It will be interesting to see whether this anomaly persists when the clean surface is covered with cesium and/or oxygen.

Cesium Adsorption. Information on the following topics is obtainable from the probe tube, (a) the variation of work function of different planes with increasing cesium adsorption, (b) the effect of electric field on the equilibrium concentration of cesium on different planes, (c) the effect of temperature on the work function of cesium on different planes, (d) migration energies of Cs along certain directions which may, in principle, be determined by depositing cesium on one side of the emitter and noting the time taken for the probe current level to change at some other point of interest.

Oxygen Adsorption. A study of $\emptyset$ versus dose number for various faces would be of interest in the case of oxygen adsorption as would an accompanying energy distribution study. Incipient oxide formation which takes place when oxygen layers on tungsten are heated above $\sim 700^{\circ}K$ may extend for a considerable depth into the substrate lattice and might be expected to have a marked change of the energy distribution results.

FIXED ORIENTATION TUBE

Work function versus cesium coverage results have usually been obtained in this work by depositing a unilateral deposit of cesium on one side of the tip and heating it until the cesium has distributed itself over the emitter. Whereas in this case, it is likely that successive doses of cesium result in proportional increases in the amounts distributed over the tip, no such conviction can be held for the amount of cesium adsorbed on any single plane. Thus the work function versus average coverage results for the 110 plane show a sharp initial decrease in work function before assuming a more gradual decline with coverage. The 100 plane on the other hand shows the

7

opposite behavior and little or no work function change is recorded for
this plane for small amounts of cesium adsorbed on the emitter. When
a cesium-covered emitter is heated to a temperature sufficient for the
cesium to be mobile and low enough so that little desorption takes place,
then the equilibrium concentration on any face will, if entropy terms are
constant, be dependent on the binding energy of cesium on that face. If
we make the assumption that on all planes the work function change is, for
small amounts of adsorption, proportional to amounts of cesium adsorbed,
then the (110) plane results indicate preferential adsorption on this plane
and the 100 plane results[2] indicate a smaller affinity of this plane for
cesium than either the 110 or the average of all of the planes on the emitter.

If some means were available for dosing all of the emitter uniformly
at low temperature, then work function versus relative coverage data would
be obtainable for individual planes and comparative dipole moments of the
adsorbed complex could be calculated for the initial stage of adsorption.
Such a dosing scheme might be effected by establishing a fixed low vapor
pressure (say 10^{-9} - 10^{-7} mm) of cesium in the field emission tube by main-
taining it and a cesium reservoir at a suitable fixed temperature in the
range 250 - 300°K. Unfortunately, the presence of cesium in a tube in
which high voltages are used, creates serious current leakage problems
so that this approach is impractical. Two other methods are available
however: the emitter may be dosed parallel to and along the emitter axis
in which case it would be necessary to assume some kind of relationship
between the concentration of cesium on a certain face and the angle θ which
the face makes with the emitter axis. Probably a cos θ fall off in con-
centration would hold. It would be possible to ascertain this by measuring
the work function change due to cesium adsorption on planes of the same
form which are situated at different angles to the emitter axis. Since work
function changes only would be required, these could be estimated without
knowledge of the electric field variation with angle θ. Use of a 310 oriented
tungsten tip would greatly facilitate the establishment of such a relationship
because of the angular position of various faces of interest. Thus a second

310 face is only 45° away from the apex 310 face; also two 110 faces at different angles of less than 90° are readily accessible.

Application of an electric field to the emitter while it is being dosed from the side results in deposition of cesium on the front and far side faces so that $\emptyset$ versus relative coverage curves can be constructed for the 100 plane in a fixed orientation probe tube. This arises from the field induced polorization of the cesium in the high field region of the emitter, thereby causing cesium deposition on the emitter side opposite the source. An example of such a curve will be discussed later.

Certain limitations are imposed by the low work function of cesium-covered surfaces and by the low ionization potential of cesium. If field emission fields are used the maximum field that can be used before excessive field emission currents are drawn is only of the order of 10 Mv/cm. At this low field value asymmetric build up of cesium on the emitter side facing the source necessitates curtailment of the $\emptyset$ versus coverage long before $\emptyset$ min. is reached. Some extension of range may be effected by reversing the field at this point since the field effect being utilized here is a function of F^2 which is of course polarity independent. The asymmetric cesium de-position soon imposes a new limit due to the fact that excessive total currents are drawn when attempts are made to obtain measureable probe currents. Higher fields of reverse polarity throughout the coverage range desired cannot be used because the low ionization potential of cesium results in gas phase field ionization of the cesium.

RESULTS

Figure 2, curve A illustrates data obtained from the 100 plane of tungsten by the above dosing procedure with a field emission field of approx-imately 16 Mv/cm. The linear decline of $\emptyset$ with dose number for this curve is in marked contrast with the similar curve B obtained by equilibrating after each dose. This data was obtained by dosing the emitter with the field off and this raises the possibility that the application of the field during dosing would have enhanced the concentration of cesium on the emitter shank. Curves C and D show that this was not the case: curve C represents average work
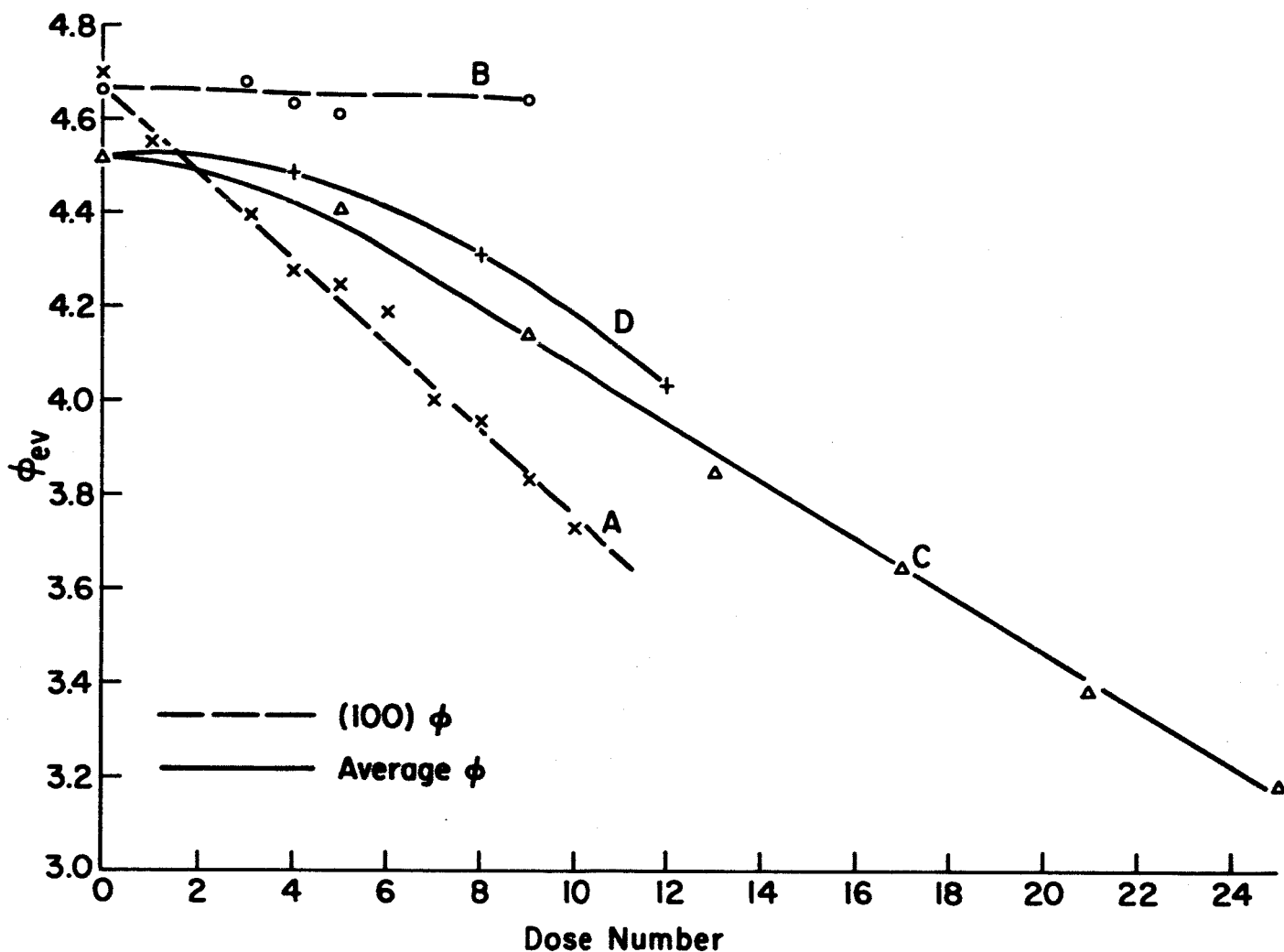
Figure 2. Work function change versus dose number for the 100 planes (curves A and B) and for the average of all planes (curves C and D).

Curve A was obtained by dosing the emitter with cesium at $78^\circ K$ with the field on.

Curve B and C were obtained by dosing with the field off and equilibrating by heating after each dose.

Curve D was obtained by dosing with the field on and equilibrating by heating after each dose.

function change resulting from an experiment involving dosing with the field off and equilibrating after each dose; no significant change took place (curve D) when this experiment was repeated with the field on during dosing.

The contrast between curves A and B seems to confirm the conclusion that the initial slow decline of $\emptyset$ with average coverage on the 100 plane is due to a relative deficiency of cesium under equilibrium conditions at low average cesium concentrations. It would be interesting to relate the concentration of cesium on the 100 plane in curve A to the average concentration represented in curve C; however no experimental information was available on this point. A crude estimate may be obtained from calculations. Certain simplifications are necessary, however: these include the assumptions that (1) the field distribution at the tip is of spherical symmetry and (2) that the cesium beam is parallel. An attempt to perform this calculation may be made in the next quarter.

It is surprising to notice that the two average $\emptyset$ vs dose plots, C and D, are curved in their initial portions whereas previously obtained average work function curves are linear in this region. The appearance of this curved region may be a consequence of the difference in dose sizes between this and earlier work. Large work function increments resulting from large cesium doses would obscure such fine grained details. The existance of the curved region is probably a manifestation of preferential adsorption of cesium on the (110) planes which at low coverages may seriously deplete all other planes of adsorbate under equilibrium conditions so that little or no work function change takes place on the lower work function planes which mostly contribute to electron emission at very low adsorbate coverages. After a small amount of cesium has been deposited, the most extreme demands of the (110) planes have been met and the average work function declines because the other planes are beginning to receive cesium and because the emission from the (110) planes is becoming an appreciable fraction of the total emission current.

ENERGY DISTRIBUTION MEASUREMENTS

In a previous report[4] we discussed a slightly different method of analyzing the integral current from retarding potential probe measurements to test the validity of the contemporary field emission theory. Recalling that the field emitted current density per unit area $J(\epsilon)$ at an energy ϵ (relative to the Fermi level, i.e., $\epsilon = E - E_f$) is given by

$$J(\epsilon) = \frac{J_o \, e^{\epsilon/d}}{d(1 + e^{\epsilon/pd})} \tag{1}$$

where $p = kT/d$ and

$$d = \frac{\hbar e F}{2(2m\emptyset)^{1/2} \, t(y)} \tag{2}$$

Under the condition $\exp(\epsilon/pd) < 1$, we observe that equation (1) can be intergrated over the limits 0 to $-\epsilon$ to yield

$$\ln \frac{I_o - I}{I_o} = \frac{\epsilon}{d} = \frac{\emptyset_c - V_c}{d} \tag{3}$$

where V_c is the tip to collector bias voltage and $\emptyset_c$ the collector work function. Alternatively under the opposite conditions in which $\exp(\epsilon/pd) > 1$, equation (1) can be integrated between the limits 0 to ϵ to give

$$\frac{p}{1-p} \ln \left[1 + \frac{I(p-1)}{I_o \, p} \right] = \frac{\epsilon}{d} \tag{4}$$

Both equations (3) and (4) can be employed to analyze portions of the I versus V_c data, i.e., equation (3) applies to emission below E_f and equation (4) applies to emission above E_f. The range of V_c over which the analysis can be made increases with decreasing value of p. In practice, equation (3) provides the most straight-forward test of the theory since the value of d is extracted directly from the plot of $\log \Delta I/I_o$ versus V_c provided a reliable value of the maximum current I_o is obtained.

We have obtained and analyzed data from the energy analyzer operating under the conditions described earlier[4]. In order to maintain accuracy the

I - V_c data was taken point by point using a Carey vibrating reed electrometer and Keithley Model 660 differential volt meter in order to maintain at least 0.5% read-out accuracy.

The resultant plot of log $\Delta I/I_o$ versus V_c for a 310 oriented emitter given in Figure 3 suggests that equation (3) is obeyed over the range of $\Delta I/I_o$ investigated for a central 310 plane. The deviation of the data from the straight line near $\Delta I/I_o = 1$ is expected since the condition $\exp(\epsilon/pd) < 1$ is no longer met and equation 3 therefore becomes seriously inaccurate. The value of the slope m_E of the straight line portion given by

$$m_E = \frac{1}{2.3\ d} \tag{5}$$

yields a value of d = 0.169 ev for an anode voltage of 1454 volts. From the value of d, which has been shown earlier to be the average energy of the field emitted electrons at $T = 0^{o}K$, the value of $\emptyset$ can be ascertained provided F is known or vice versa. Table I gives values of m_E for other 310 directions obtained by magnetically deflecting the beam so the desired plane was centered on the probe hole of the analyzer tube. Since the electric field strength decreases with increasing angle from the apex of the emitter, one expects m_E to increase with θ. Instead, m_E decreases slightly which suggests the magnetic field employed to deflect the beam affects the operation of the analyzer tube even though great care was taken to concentrate the magnetic field to the emitter region.

WORK FUNCTION MEASUREMENTS

In the previous report[4] we discussed three weaknesses in the "Fowler-Nordheim" (FN) slope method for determining local work function values. First, the method is relative so that even the average work function or the work function of a particular plane from which the I-V data is obtained must be determined from other methods. Second, because of the emitter shape, the field decreases with increasing angle from the apex; this must be reckoned with in the work function evaluation. Thirdly, besides the overall uniform
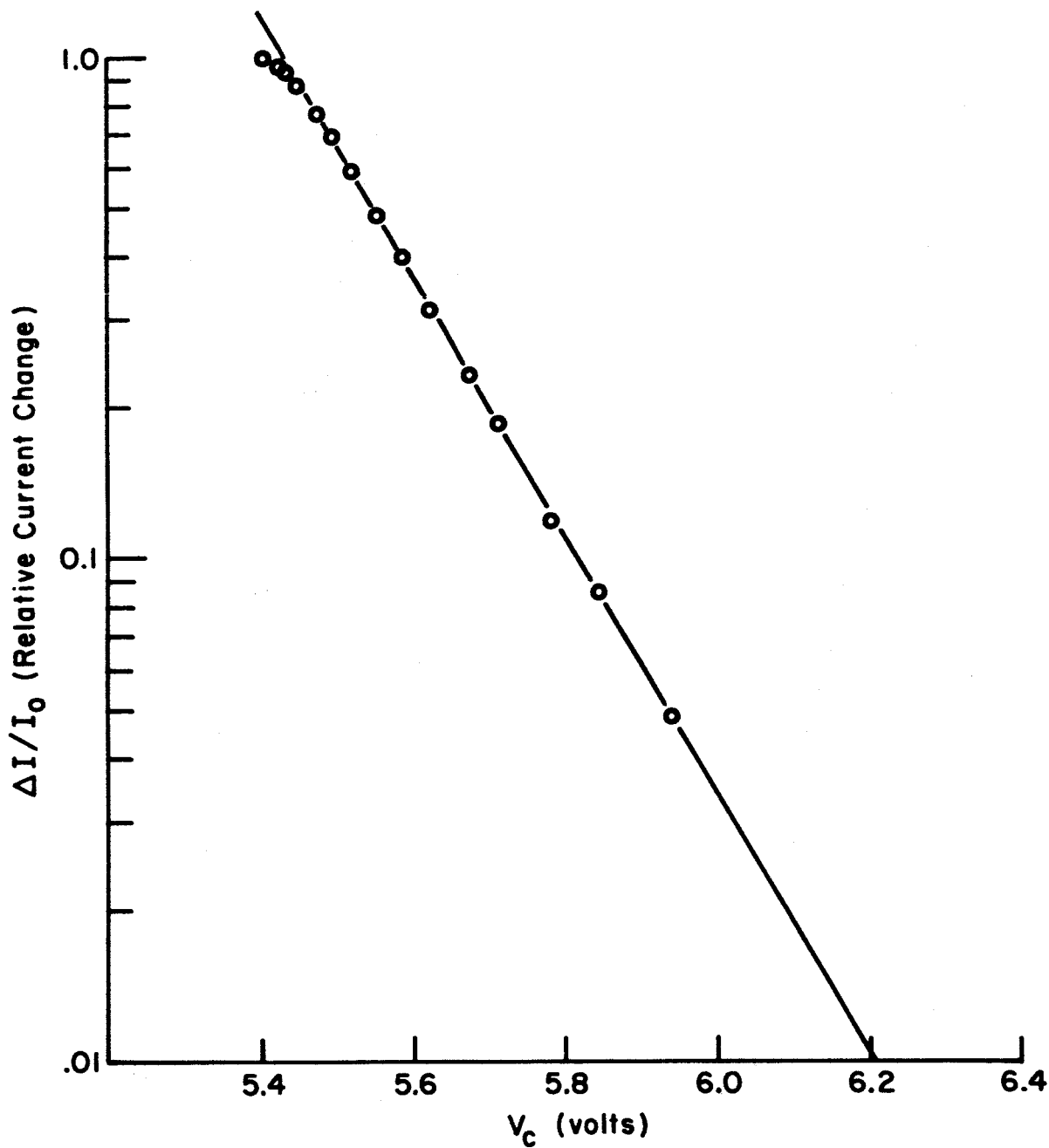
13

Figure 3. Plot of log $\Delta I/I_o$ vs. tip-to-collector bias voltage according to equation (3) for a 310 oriented tungsten emitter. Anode voltage 1454 volts.

variation of field, there are also local variations from plane to plane due to local faceting of the emitter. For example, the normal thermodynamically stable end form of a tungsten emitter possesses relatively large 110 and 112 crystal faces.

As mentioned previously[4], the second weakness of the FN slope method mentioned above can be overcome to some extent by utilizing a numerical calculation[5] for the field variation over a typically shaped field emitter. Such a relation between the variation of field with apex angle θ is given in Figure 4. A rough check of the correctness of the curve given in Figure 4 was obtained from a $\langle 310 \rangle$ oriented emitter by measuring the I-V characteristics for the $\langle 310 \rangle$, $\langle 130 \rangle$, $\langle 3\bar{1}0 \rangle$ and $\langle \bar{1}30 \rangle$ directions. Recalling that the slope m_F of the FN plot is related to the field factor β and work function $\emptyset$ as follows

$$m_F = \frac{b \, \emptyset^{3/2}}{\beta} \tag{6}$$

where $F = \beta V$; making the reasonable assumption that each of the above-mentioned planes have the same work function, then the ratio of the FN slope $m_F(\theta)$ of the plane whose normal makes an angle θ from the apex is given by

$$\frac{F(\theta)}{F_o} = \frac{\beta(\theta)}{\beta_o} = \frac{m_o}{m_F(\theta)} \tag{7}$$

where m_o, β_o, and F_o refer to the $\langle 310 \rangle$ direction along the emitter axis.

The most recent data points obtained in this fashion are plotted in Figure 4 according to equation 7. The deviation of the data points from the assumed curve does not exceed 2%, which is within the accuracy of the FN plots. We therefore conclude that the corrections to the work function calculations based on the average emitter shape curve of Figure 4 are reasonably correct. Thus one of the three major uncertainties of the FN slope method for determining work functions of various crystal phases is removed.

We have also plotted in Figure 4 the variation of relative linear magnification M_{rel} versus θ. The linear magnification M is related to the area of the probe
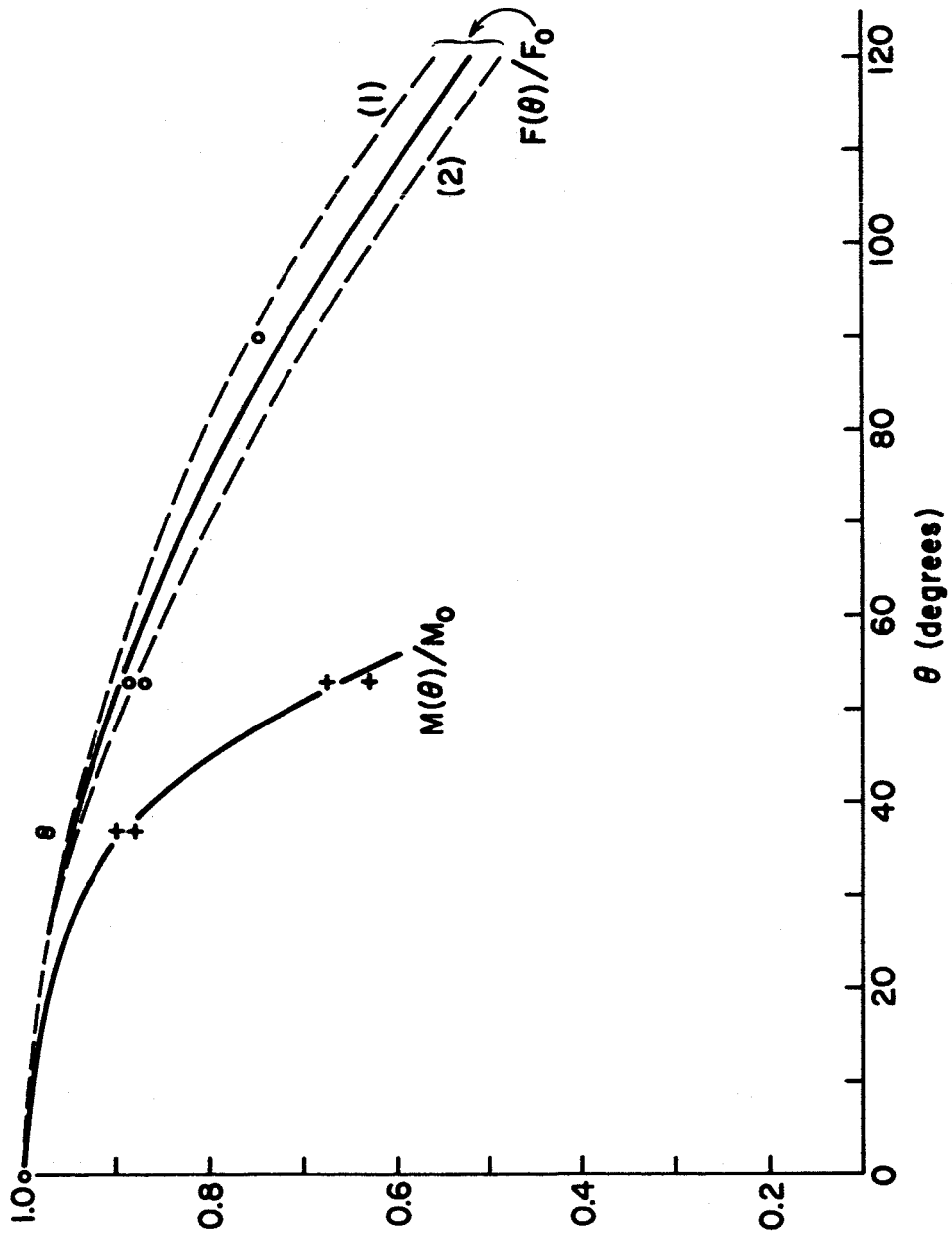
Figure 4. $F(\theta)/F_o$ is the relative variation of electric field with angular distance from θ emitter apex. Dashed curves: (1) emitter with pronounced constriction; (2) emitter with slight constriction; solid line for average emitter shape. Experimental data for $F(\theta)/F$ given by circles. Lower curve gives the relative variation of magnification with θ; data points indicated by crosses.

hole A_p and the emitting area A seen by the probe as follows:

$$M = \left(\frac{A_f}{A}\right)^{1/2} \qquad (8)$$

The emitting area can be obtained directly from the experimental inter-cepts B of the FN plots by noting

$$B = \frac{C A \beta^2}{\emptyset} \qquad (9)$$

where C is a constant. Whence according to equations (8) and (9) the magnification at an angle θ from the emitter axis relative to the mag-nification along the emitter axis is given by

$$M_{rel} = \left(\frac{A_o}{A(\theta)}\right)^{1/2} \frac{\beta(\theta)}{\beta_o} \qquad (10)$$

The values of M_{rel} decreases more rapidly with θ than $F(\theta)/F_o$ (which is identical to $\beta(\theta)/\beta_o$) as expected. At larger angles, M_{rel} as deter-mined by this method, is probably not reliable because of possible com-pression or expansion of the beam by the deflecting magnetic field.

Another method of ascertaining both the absolute work function and local value of β of a single crystal plane which circumvents all previously mentioned problems is available within the framework of contemporary field emission theory. The slope m_E of a plot of $\Delta I/I_o$ versus V_c as given in equation (3) yields the value of d; this experimental slope when combined with the FN slope, equation (6), leads to an expression from which the absolute work function can be obtained.

$$\emptyset = \frac{3}{2} \frac{m_E}{m_F} \frac{t(y)}{V s(y)} \qquad (11)$$

Thus, the absolute work function and β can be ascertained from simultan-eous energy distribution and FN measurements. The values of $\emptyset$ obtained in this fashion can be compared with work functions obtained by other methods thus providing perhaps the most stringent tests of field emission theory.

The values of $\emptyset$ obtained by equation (11) are given in Table I for three 310 planes at different angles from the emitter axis. The value of $\emptyset$ along the emitter axis (no magnetic field applied) is 4.85 ev as compared to a value of 4.30 ev obtained from a comparison between the Fowler-Nordheim slopes of the total and probe currents, assuming an average work function of 4.52 ev. For the 37° (310) plane, a slightly higher value of $\emptyset$ is obtained probably because of the perturbing influence of the deflecting magnetic fields on the energy distribution measurement. Similarly, the 53° (310) plane gives a value of $\emptyset$ much too large because of the erroneous value of m_E. Whether the difference between the 4.85 ev work function obtained by equation 11 and the 4.30 ev work function obtained by the Fowler-Nordheim slope method is due to experimental error or to a slight deviation in m_E from theory cannot be stated absolutely until additional data is obtained from other crystallographic directions. However, we are inclined to believe, particularly in view of the deviation of the $\langle 100 \rangle$ direction energy distribution results from theory[6], that equation (1) is not exactly obeyed by tungsten because of its marked deviation from free electron theory.

TABLE I

Calculation of $\emptyset$ according to equation (11) for various $\langle 310 \rangle$ planes on a $\langle 310 \rangle$ oriented emitter at an anode voltage of 1454 volts.

Angel from apex	I_o $(\times 10^{-10}$ amps)	m_E (volts^{-1})	m_F/m_E $(\times 10^3$ volts)	$\emptyset$ (ev)
0°	2.48	2.580	4.339	4.85
37°	1.85	2.558	4.443	4.97
53°	0.40	2.255	5.602	6 26

REFERENCES

1. L. W. Swanson, et al, Quarterly Report No. 2 for NASA Contract NASw-1082 (Field Emission Corporation, 1965).

2. L. W. Swanson, et al, Annual Report for NASA Contract NASw-458 (Field Emission Corporation, 1965).

3. L. W. Swanson, et al, Quarterly Report No. 1 for NASA Contract NASw-1082 (Field Emission Corporation, 1965).

4. L. W. Swanson, et. al., Quarterly Report No. 4 for NASA Contract NASw-1082 (Field Emission Corporation, 1965).

5. W. P. Dyke, et al., Journal of Applied Physics, 24, 570, (1953).

6. L. W. Swanson, et. al., Quarterly Report No. 3 for NASA Contract NASw-1082 (Field Emission Corporation, 1965).